

Dahl Hysteresis Modeling and Position Control of Piezoelectric Digital Manipulator

Gerardo Flores^{ID}, Member, IEEE, and Micky Rakotondrabe^{ID}, Member, IEEE

Abstract—The synthesis of a feedback controller based on a hysteresis model is challenging, mainly when the hysteresis is non-symmetric. In this letter, we propose to model a non-symmetric hysteresis of a piezoelectric actuator by using the Dahl model and design a nonlinear feedback controller for the system. For that aim, we exploit the boundedness of the system states to design an extended observer responsible for estimating the part of the system that is observable, including non-modeled terms and exogenous signals. Then, we design active disturbance rejection control that globally asymptotically stabilizes the tracking error. Finally, simulations were carried out to demonstrate the effectiveness of our approach.

Index Terms—Dahl hysteresis model, asymmetric hysteresis control, piezoelectric system, active disturbance rejection control (ADRC), nonlinear and extended observer.

I. INTRODUCTION

PIEZOELECTRIC actuators use the converse piezoelectric effect as a fundamental principle: an electrical field applied to the piezoelectric material results in its mechanical deformation. This material deformation or its amplified value will correspond to the exploitable displacement the piezoelectric actuator will provide for the application use. Because the deformation is continuous, piezoelectric actuators are typified by a very high resolution (down to nanometers) which makes them widely used in applications that require precise positioning, such as medical surgery based on microrobotics [1], diesel injection in recent engines [2], data storage with hard disk [3], or precise imaging based on scanning probe microscopy [4]. In counterpart, piezoelectric actuators can exhibit hysteresis nonlinearity because the material is also ferroelectric. When the applied electrical field induced by a driving voltage is chosen to be large to increase the output displacement, the hysteresis

Manuscript received 16 September 2022; revised 18 November 2022; accepted 2 December 2022. Date of publication 20 December 2022; date of current version 29 December 2022. This work was supported in part by the Laboratorio Nacional de Supercómputo del Sureste de México (LNS) under Agreement 202201026N. Recommended by Senior Editor G. Cherubini. (*Corresponding author:* Gerardo Flores.)

Gerardo Flores is with the Laboratorio de Percepción y Robótica, Center for Research in Optics, León 37150, Mexico (e-mail: gflores@cio.mx).

Micky Rakotondrabe is with the Laboratoire Génie de Production, National School of Engineering in Tarbes (ENIT-INPT), University of Toulouse, 65000 Tarbes, France (e-mail: mrakoton@enit.fr).

This article has supplementary downloadable material available at <https://doi.org/10.1109/LCSYS.2022.3230472>, provided by the authors.

Digital Object Identifier 10.1109/LCSYS.2022.3230472

phenomenon becomes strong, and the overall performances, such as task accuracy, are no longer ensured.

The literature is abundant regarding the control of piezoelectric actuators with hysteresis. They can be classified into feedforward and feedback architectures. Feedforward architecture consists of modeling as precisely as possible the hysteresis and using an inverse of the model or an approximate or equivalent operator of the inverse model as a controller placed in cascade with the system. Those models principally include Bouc-Wen models, Prandtl-Ishlinskii models and Preisach models [5], [6], [7]. While the main reason to use feedforward is the unavailability of appropriate sensors in certain applications and the low cost, it lacks robustness against external disturbances and model uncertainties. Hence, feedback architecture is generally suggested as soon as employing a sensor is possible. In feedback control of piezoelectric actuators, three subcategories can be found: i) synthesis of the controller without a hysteresis model, ii) synthesis of the controller on the basis of a linear model after compensating for the hysteresis, and iii) synthesis of the controller with a direct hysteresis model. The former uses an approximate and simple model (linear...) and allows to apply of standard control techniques (PID with Ziegler-Nichols, RST, H_∞ , ...) [8] but finds its limit as soon as the hysteresis amplitude becomes large when the driving voltage increases. The second consists in compensating for the hysteresis first (inverse feedforward, disturbance observer rejection...), and then computing the controller afterwards with a more straightforward and linearized model [9]. Finally, for the third case, where the feedback controller is directly designed using an explicit model of the hysteresis, fewer works than above cases have been carried out due to the complexity of the model itself to be accounted for in the feedback design [10]. This letter lies within this third subcategory. In [11], the classical Bouc-Wen model was used to design an output feedback controller and a nonlinear observer to guarantee global exponential stability of the piezoelectric actuator. However, the classical Bouc-Wen model can approximate symmetric hysteresis only, and the feedback instability could occur if the synthesized controller is applied to an actuator with non-symmetric hysteresis. To account for hysteresis asymmetry, we proposed to use the generalized Bouc-Wen model along with we synthesized a model predictive controller in [12], and then a nonlinear output feedback controller for finite time stabilization in [13]. Another model that can account for non-symmetric hysteresis is the Dahl model. This

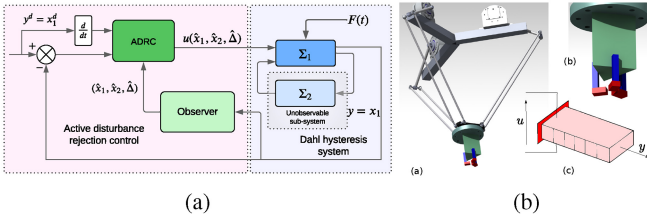


Fig. 1. a) The block diagram of the closed-loop system. Subsystem Σ_2 is unobservable and contains the hysteresis dynamics. The only available state is the position $y = x_1$. See model (1a) and ADRC (35). The observer estimates all the system states and the unknown term $\Delta(t)$. b) A parallel robot with a hand with three fingers, each of which is a piezoelectric actuator.

latter model is known to provide better precision than the generalized Bouc-Wen model when approximating non-symmetric hysteresis thanks to its structure [14]. In this regard, in [15], the authors design an SMC to track the desired position trajectory using a second-order Dahl model; they used an approximation of the hysteresis term, which is feedforwarded in the control input since the actual hysteresis value is not available for feedback.

In this letter, we propose to employ the Dahl hysteresis model to describe the piezoelectric actuator's hysteresis and design a feedback controller to ensure its stability. Please refer to Fig. 1 for a graphic abstract of the contribution. The studied actuator itself is one of the actuators that compose a robotic hand devoted to precise manipulation of deformable or fragile objects [16], each actuator being called a digital finger or manipulator. With that aim, we first study the states' behavior under bounded inputs proving that all the states remain bounded. Such a condition helps design an extended observer to estimate the position and velocity of the manipulator together with the disturbance response. Once such estimates are given, we design an active disturbance rejection control with a scheme of output feedback control. The closed-loop system with the proposed controller is globally asymptotically stable. All these results are rigorously mathematically proven. Contrary to the work in [15], we propose in this letter to estimate the hysteresis state of the Dahl model, explicitly use it for feedback, and demonstrate the global asymptotic stability of the closed-loop.

The remainder of this letter is as follows. In Section II, the mathematical model of the piezoelectric digital manipulator is described. Besides, we present the problem statement. In Section III we design the control algorithm consisting of three main propositions. We follow a proposed procedure to achieve global asymptotic stability in the closed-loop system by using only position measurements of the piezoelectric digital manipulator. Then, in Section IV we present numerical simulations that corroborate the closed-loop system convergence. Finally, some comments and conclusions are given in Section V.

II. MODELING AND PROBLEM STATEMENT

The robotic hand, as well as the three piezoelectric actuators that compose it, are detailed in previous work [16]. In this letter, we focus on one single actuator (digital manipulator).

The actuator model when with hysteresis, is given by:

$$m_p \ddot{x} = -c_p \dot{x} - k_p x + d_p u - h - F \quad (1a)$$

$$\Sigma : \begin{cases} h = \gamma \operatorname{sgn}(\dot{x}) z \\ \dot{z} = -\alpha \dot{x} - \beta |\dot{x}| z \end{cases} \quad (1b)$$

$$(1c)$$

and the output of interest is the displacement:

$$y = x \quad (2)$$

where: x is the piezoelectric actuator's displacement, u is the driving voltage acting as the only control input, F is an external and unknown force applied by the environment to the actuator (manipulated object or other environmental conditions), and h is a friction-like that resists the movement nonlinearly to create the hysteresis. The friction h depends on an internal hysteresis state z and the velocity \dot{x} .

Equation (1a) represents the dynamics of the actuator's mechanical part and is similar to whether we use the Bouc-Wen model or the Dahl model. Equations (1b)-(1c) are proper to the Dahl model, see for instance [14], [17]. Beyond the accuracy of the Dahl model over the generalized Bouc-Wen model to approximate asymmetric hysteresis, we choose it because it can reflect more on the physical phenomenon within the piezoelectric material. Indeed, the hysteresis of the piezoelectric material is due to friction between Weiss domains within the material, which align with the applied electrical field. We, therefore, represent the hysteresis with a model successfully used in friction.

All parameters are [14], [17]:

- m_p , c_p and k_p are the equivalent mass, the equivalent damper coefficient and the equivalent stiffness of the actuator,
- d_p is the voltage-to-force homogenization coefficient,
- γ , α , and β are parameters that define the hysteresis size.

Notice that all the system parameters are considered positive. In the sequel, we will consider the external force F as a disturbance to be rejected. The problem is stated as follows.

Problem 1: Given system Σ in (1a), the goal is to solve the position tracking problem by proposing a control law that only uses the output (2) for feedback. Besides, the control law must cope with exogenous and unknown signal $F(t)$ in (1a) and achieve asymptotic stability.

III. CONTROL

The control strategy consists of the following steps:

- 1) Analyze the system Σ to determine the states' behavior. At this point, we hypothesize that the states (x, \dot{x}, z) remain bounded globally, but this will be demonstrated further in this letter.
- 2) Since the subsystem (1c) represents the state equation of the friction-like phenomenon, we will consider the term $-\gamma \operatorname{sgn}(\dot{x}) z - F := \Delta(x, \dot{x}, z, t)$ as a disturbance including unmodeled terms and exogenous forces.
- 3) We design an observer to estimate the terms (x, \dot{x}, Δ) and use them for feedback when designing the control for subsystem (1a).
- 4) Finally, we design an output-feedback and active disturbance rejecting control $u(x, \dot{x}, \hat{\Delta})$ for solving the position tracking problem expressed in Problem 1.

Our control design strategy requires that the solutions of Σ_2 are bounded since it is impossible to access or control such a system. By proving that (x_1, x_2, z) are bounded (under bounded inputs), we can conclude that the Σ_2 solutions are bounded, as demonstrated in the following Lemma.

Assumption 1: The external and unknown force $F(t)$ in (1a) is bounded by $|F(t)| \leq \delta_x$, where $\delta_x \in \mathbb{R}_{\geq 0}$.

Lemma 1: Let us rewrite system Σ as follows,

$$\Sigma_1 : \begin{cases} \dot{x}_1 = x_2 \\ \dot{x}_2 = -\frac{k_p}{m_p}x_1 - \frac{c_p}{m_p}x_2 + \frac{d_p}{m_p}u \\ \underbrace{-\frac{\gamma}{m_p}\text{sgn}(x_2)z - \frac{1}{m_p}F(t)}_{\Delta(t)} \end{cases} \quad (3a)$$

$$\Sigma_2 : \{\dot{z} = -\alpha x_2 - \beta |x_2|z\}. \quad (4a)$$

where $x_1 = x$, $x_2 = \dot{x}$. Besides, consider that Assumption 1 holds and the control input u in the system above is bounded as $|u| \leq \sup\{|u(t)|\}_{t \geq 0} = \mu \in \mathbb{R}_{\geq 0}$. Then, all the solutions of (3a)-(4a) are uniformly bounded.

Proof: Let us propose the following candidate Lyapunov function $V_o = \frac{\lambda}{2}x_1^2 + x_1x_2 + \frac{q}{2\lambda}x_2^2 + \frac{1}{2}z^2$ with $\lambda > 0$, and $q > 1$. Such a function is positive definite, it can be easily verified by rewriting it as $V_o = x^T P x$ with $x = [x_1, x_2, z]^T$, and $P = \begin{pmatrix} \frac{\lambda}{2} & \frac{1}{\lambda} & 0 \\ \frac{1}{\lambda} & \frac{q}{2\lambda} & 0 \\ 0 & 0 & \frac{1}{2} \end{pmatrix}$. Since all the upper left determinants of P are positive as long as $\lambda > 0$, and $q > 1$, it is clear that $V_o > 0$. The time-derivative of V_o is computed as follows,

$$\begin{aligned} \dot{V}_o &= \lambda x_1 x_2 + \left(x_1 + \frac{q}{\lambda}x_2\right)\left(-\frac{k_p}{m_p}x_1 - \frac{c_p}{m_p}x_2\right. \\ &\quad \left.- \frac{\gamma}{m_p}\text{sgn}(x_2)z + \frac{d_p}{m_p}u - \frac{1}{m_p}F(t)\right) + x_2^2 \\ &\quad + z(-\alpha x_2 - \beta |x_2|z). \end{aligned} \quad (5)$$

From the conditions of this Lemma, it follows that $|d_p u - F(t)| \leq d_p \mu + \delta_x = \theta \in \mathbb{R}_{\geq 0}$. Thus, (5) is,

$$\begin{aligned} \dot{V}_o &\leq \lambda x_1 x_2 - \frac{k_p}{m_p}x_1^2 - \frac{c_p}{m_p}x_1 x_2 - \frac{\gamma}{m_p}\text{sgn}(x_2)x_1 z \\ &\quad + \frac{\theta}{m_p}|x_1| + x_2^2 + \frac{q}{\lambda}\left(-\frac{k_p}{m_p}x_1 x_2 - \frac{c_p}{m_p}x_2^2\right. \\ &\quad \left.+ \frac{\gamma}{m_p}|x_2||z| + \frac{\theta}{m_p}|x_2|\right) + \alpha|x_2||z| - \beta|x_2|z^2. \end{aligned} \quad (6)$$

which can be simplified as follows,

$$\begin{aligned} \dot{V}_o &\leq -\frac{k_p}{m_p}x_1^2 - \left(\frac{c_p q}{m_p \lambda} - 1\right)x_2^2 - \beta|x_2|z^2 \\ &\quad + \left(\lambda - \frac{c_p}{m_p} - \frac{k_p q}{m_p \lambda}\right)x_1 x_2 + \frac{\gamma}{m_p}|x_1||z| \\ &\quad + \left(\frac{\gamma q}{m_p \lambda} + \alpha\right)|x_2||z| + \frac{\theta}{m_p}|x_1| + \frac{\theta q}{m_p \lambda}|x_2|. \end{aligned} \quad (7)$$

We solve the equation $\lambda - \frac{c_p}{m_p} - \frac{k_p q}{m_p \lambda} = 0$ for $\lambda > 0$, and $q > 1$, and then,

$$\begin{aligned} \dot{V}_o &\leq -\frac{k_p}{m_p}x_1^2 - \left(\frac{c_p q}{m_p \lambda} - 1\right)x_2^2 - \beta|x_2|z^2 + \frac{\gamma}{m_p}|x_1||z| \\ &\quad + \left(\frac{\gamma q}{m_p \lambda} + \alpha\right)|x_2||z| + \frac{\theta}{m_p}|x_1| + \frac{\theta q}{m_p \lambda}|x_2|. \end{aligned} \quad (8)$$

We apply the Young inequality to the positive cross terms as follows,

$$\begin{aligned} \frac{\gamma}{m_p}|x_1||z| &\leq \frac{1}{2}\frac{\gamma^2}{m_p^2} + \frac{1}{2}x_1^2 z^2, \\ \left(\frac{\gamma q}{m_p \lambda} + \alpha\right)|x_2||z| &\leq \frac{1}{2}\left(\frac{\gamma q}{m_p \lambda} + \alpha\right)^2 + \frac{1}{2}x_2^2 z^2, \\ \frac{\theta}{m_p}|x_1| + \frac{\theta q}{m_p \lambda}|x_2| &\leq \frac{1}{2}\frac{\theta^2}{m_p^2} + \frac{1}{2}x_1^2 + \frac{1}{2}\left(\frac{\theta q}{m_p \lambda}\right)^2 + \frac{1}{2}x_2^2. \end{aligned} \quad (9)$$

From (9), (8) is expressed as,

$$\begin{aligned} \dot{V}_o &\leq -\left(\frac{k_p}{m_p} - \frac{1}{2}z^2 - \frac{1}{2}\right)x_1^2 - \left(\frac{c_p q}{m_p \lambda} - \frac{1}{2}z^2 - \frac{3}{2}\right)x_2^2 \\ &\quad - \beta|x_2|z^2 + \underbrace{\frac{1}{2}\left(\frac{\gamma^2}{m_p^2} + \left[\frac{\gamma q}{m_p \lambda} + \alpha\right]^2 + \frac{\theta^2}{m_p^2} + \frac{\theta^2 q^2}{m_p^2 \lambda^2}\right)}_r. \end{aligned} \quad (10)$$

Notice that $\dot{V}_o - r \prec 0 \quad \forall x_1, x_2 \text{ and } |z| \leq \min\{\sqrt{2\frac{k_p}{m_p} - 1}, \sqrt{2\frac{c_p q}{m_p \lambda} - 3}\}$ with $\frac{k_p}{m_p} > \frac{1}{2}$, and $\frac{c_p}{m_p} > \frac{3\lambda}{2q}$. Then,

$$\dot{V}_0 \leq -\psi \|x\|^2 + L \quad (11)$$

in a region near the origin that includes it, where $L \in \mathbb{R}_{>0}$, $\psi \in (0, 1)$ and $L > r$. Such a region can be arbitrarily large by choosing the parameters ψ and L .

Now, let us consider $M := \frac{\psi}{\lambda_{\max}\{P\}}$. And $x = [x_1, x_2, z]^T$ be any solution of system Σ with initial condition $x_0 = x(t_0) \forall t \geq t_0$. To prove that the solutions of Σ under bounded disturbance and control are bounded, notice that

$$\frac{d}{dt}(V_o(x)e^{M(t-t_0)}) = (\dot{V}_o(x)e^{M(t-t_0)} + MV_o(x)e^{M(t-t_0)}), \quad (12)$$

and when we substitute (11) in the expression above, it follows that,

$$\frac{d}{dt}(V_o(x)e^{M(t-t_0)}) \leq (-\psi \|x\|^2 + L + MV_o(x))e^{M(t-t_0)}. \quad (13)$$

Notice that due to the positive definitiveness of $V_o(x)$, the expression:

$$\lambda_{\min}\{P\}\|x\|_2^2 \leq V_o(x) \leq \lambda_{\max}\{P\}\|x\|_2^2 \quad (14)$$

holds. By substituting the right-hand side of (14) into (13) and using the definition of M , it follows that,

$$\begin{aligned} \frac{d}{dt}(V_o(x)e^{M(t-t_0)}) &\leq \left(-\frac{\psi V_o(x)}{\lambda_{\max}\{P\}} + L + MV_o(x)\right)e^{M(t-t_0)} \\ &\leq Le^{M(t-t_0)}. \end{aligned} \quad (15)$$

We integrate both sides of (15) from t_0 to t and one gets,

$$V_o(x)e^{M(t-t_0)} - V_o(x_0) \leq \frac{L}{M}e^{M(t-t_0)} - \frac{L}{M}, \quad (16)$$

and from the right-hand side of (14) the expression above is expressed as,

$$V_o(x)e^{M(t-t_0)} \leq \lambda_{\max}\{P\}\|x_0\|_2^2 + \frac{L}{M}\left(e^{M(t-t_0)} - 1\right). \quad (17)$$

After some computations, it follows that,

$$V_o(x) \leq \lambda_{\max}\{P\}\|x_0\|_2^2 e^{-M(t-t_0)} + \frac{L}{M}. \quad (18)$$

Using the left-hand side of (14) it follows that,

$$\lambda_{\min}\{P\}\|x\|_2^2 \leq \lambda_{\max}\{P\}\|x_0\|_2^2 e^{-M(t-t_0)} + \frac{L}{M}. \quad (19)$$

Finally,

$$\|x\| \leq \left(\frac{1}{\lambda_{\min}^{1/2}\{P\}}\right)\left(\lambda_{\max}\{P\}\|x_0\|_2^2 + \frac{L}{M}\right)^{1/2}, \quad \forall t \geq t_0. \quad (20)$$

Since $V_o : \mathbb{R}^3 \rightarrow \mathbb{R}_{>0}$, all the solutions of the system Σ are uniformly bounded. ■

A. Observer

By the notation used in (3a), subsystem Σ_1 appears as a second-order system perturbed by $\Delta(t)$. Therefore, $\Delta(t)$ is considered unknown as part of our control design. This way, we get that the z state does not directly appear in the subsystem Σ_1 , and thus we eliminated the need for designing a full-state observer. The latter is feasible because all the states of the complete system Σ are bounded (see Lemma 1). With the above discussion, it is possible designing an observer for (x_1, x_2) just considering subsystem Σ_1 in (3a) setting aside the subsystem Σ_2 in (4a), which models the internal hysteresis behavior. The primary motivation for the above approach is that Σ_2 is not observable, as explained next, where the complete system's observability is studied.

Recall that the only available output is given by the position state x_1 , as described by (2). In this sense, it is easy to conclude that the system (Σ_1, Σ_2) is not observable. For that, assume that the initial state $z_0 = z(t_0)$ is unknown. If the state x_1 and input u are available over a finite time $[t_0, t_1]$ for an arbitrary time $t_1 > t_0$, it is not possible to determine uniquely z_0 . In particular, when $x_2 = 0$, (4a) results in $\dot{z}(t) = 0$, and no matter if we know the pair (x_1, u) , it is not possible to recover the initial state z_0 . However, the system Σ_1 with output (2) is observable as demonstrated in the following lemma.

Lemma 2: The system Σ_1 with output $y = x_1$ is observable.

Proof: Let us rewrite system Σ in (3a) as,

$$\dot{\bar{x}} = \bar{A}\bar{x} + \bar{B}\left(\frac{\Delta + d_p u}{m_p}\right), \quad y = \bar{C}\bar{x}, \quad (21)$$

with $\bar{x} = [x_1, x_2]^\top$, $\bar{A} = \begin{pmatrix} 0 & 1 \\ -\frac{k_p}{m_p} & -\frac{c_p}{m_p} \end{pmatrix}$, $\bar{B} = [0, 1]^\top$, and $\bar{C} = [1, 0]$. Since all the system parameters are positive, it is forward to verify that the pair (\bar{A}, \bar{C}) is full rank. ■

The extended state observer is presented in the following proposition.

Proposition 1: Let us consider system Σ_1 with exogenous signal $\Delta(x_1, x_2, z, t)$ in (3a). Since all the system states, control, and disturbance in (Σ_1, Σ_2) are bounded by Lemma 1, the following system is an observer for Σ_1 and $\Delta(x_1, x_2, z, t)$,

$$\begin{aligned} \dot{\hat{x}}_1 &= \hat{x}_2 - l_1(\hat{x}_1 - x_1) \\ \dot{\hat{x}}_2 &= -\frac{k_p}{m_p}\hat{x}_1 - \frac{c_p}{m_p}\hat{x}_2 + \frac{d_p}{m_p}u + \hat{\Delta} - l_2(\hat{x}_1 - x_1) \\ \dot{\hat{\Delta}} &= -l_3 \frac{\hat{x}_1 - x_1}{|\hat{x}_1 - x_1| + \epsilon} - l_4\hat{\Delta} \end{aligned} \quad (22)$$

with $l_i \in \mathbb{R}_{>0}$ for $i = \{1, 2, 3\}$, $\epsilon < 0 \in \mathbb{R}_{>0}$, and inequalities,

$$l_1 > l_2 + \frac{k_p}{m_p} + \frac{l_3}{\epsilon}, \quad \frac{c_p}{m_p} > 1, \quad l_4 > \frac{1 + c_1 c_2}{1 - c_1}. \quad (23)$$

Then, the observer errors,

$$e_1 = \hat{x}_1 - x_1, \quad e_2 = \hat{x}_2 - x_2, \quad e_3 = \hat{\Delta} - \Delta, \quad (24)$$

such that the disturbance and its first-time derivative are bounded by,

$$|\Delta(x, t)| \leq c_1|e_3|, \quad |\dot{\Delta}(x, t)| \leq c_2|e_3|, \quad (25)$$

with $\mathbb{R}_{>0}$, globally exponentially converge to the origin.

Proof: First, let us compute the first-time derivative of the errors (24) along the solutions of system (3a) and observer (22) as follows,

$$\begin{aligned} \dot{e}_1 &= e_2 - l_1 e_1 \\ \dot{e}_2 &= -\left(l_2 + \frac{k_p}{m_p}\right)e_1 - \frac{c_p}{m_p}e_2 + e_3 \\ \dot{e}_3 &= -l_3 \frac{\hat{x}_1 - x_1}{|\hat{x}_1 - x_1| + \epsilon} - l_4\hat{\Delta} - \dot{\Delta}(x, t). \end{aligned} \quad (26)$$

Let us propose the following candidate Lyapunov function $W = |e_1| + |e_2| + |e_3|$ with first-time derivative along the error solutions (26) given by,

$$\begin{aligned} \dot{W} &= \text{sgn}e_1(\dot{e}_1) + \text{sgn}e_2(\dot{e}_2) + \text{sgn}e_3(\dot{e}_3) \\ &= \text{sgn}e_1(e_2 - l_1 e_1) + \text{sgn}e_2\left(-\left[l_2 + \frac{k_p}{m_p}\right]e_1\right. \\ &\quad \left.- \frac{c_p}{m_p}e_2 + e_3\right) + \text{sgn}e_3\left(-l_3 \frac{e_1}{|e_1| + \epsilon} - l_4\hat{\Delta} - \dot{\Delta}\right) \\ &\leq -\left(l_1 - l_2 - \frac{k_p}{m_p} - \frac{l_3}{\epsilon}\right)|e_1| - \left(\frac{c_p}{m_p} - 1\right)|e_2| \\ &\quad - (l_4 - l_4 c_1 - c_2 - 1)|e_3|, \end{aligned} \quad (27)$$

since $\frac{l_3}{|e_1| + \epsilon} \leq \frac{l_3}{\epsilon}$. Thus, (27) is clearly negative definite when the inequalities in (23) hold. And since $\dot{W} \leq -aW$ for $a = \min\{l_1 - l_2 - \frac{k_p}{m_p} - \frac{l_3}{\epsilon}, \frac{c_p}{m_p} - 1, l_4 - l_4 c_1 - c_2 - 1\}$ the error equilibrium point (24) is globally exponentially stable. ■

B. Control

Recall that we have demonstrated in Lemma (1) that all the states of system (Σ_1, Σ_2) remain bounded. Since the goal is that x_1 tracks a desired signal x_1^d , we focus on controlling subsystem Σ_1 . Next, we present part of the main result.

Proposition 2: Let $(x_1^d, x_2^d = \dot{x}_1^d)$ be time-varying desired bounded trajectories for subsystem Σ_1 . Then, the control law,

$$\begin{aligned} u(x_1, x_2, \Delta) &= \frac{m_p}{d_p} \left(\frac{k_p}{m_p} [\varepsilon_1 + x_1^d] + \frac{c_p}{m_p} [\varepsilon_2 + x_2^d] - \Delta(x, t) \right. \\ &\quad \left. + \dot{x}_2^d - [k_1 k_2 + 1] \varepsilon_1 - [k_1 + k_2] \varepsilon_2 \right) \end{aligned} \quad (28)$$

where $k_1, k_2 \in \mathbb{R}_{>0}$, globally exponentially stabilize the error origin:

$$\varepsilon_1 = x_1 - x_1^d, \quad \varepsilon_2 = x_2 - x_2^d \quad (29)$$

for system Σ_1 in (3a).

Proof: Let us consider the change of coordinates,

$$\xi_1 = \varepsilon_1, \quad \xi_2 = \varepsilon_2 - v \quad (30)$$

where v is a virtual control to be defined. Then, (30) has dynamics,

$$\begin{aligned} \dot{\xi}_1 &= \xi_2 + v \\ \dot{\xi}_2 &= -\frac{k_p}{m_p} (\xi_1 + x_1^d) - \frac{c_p}{m_p} (\xi_2 + v + x_2^d) \\ &\quad + \frac{d_p}{m_p} u + \Delta(x, t) - \dot{x}_2^d - \frac{\partial v}{\partial \xi_1} \dot{\xi}_1 - \frac{\partial v}{\partial \xi_2} \dot{\xi}_2. \end{aligned} \quad (31)$$

Let us define $V_1 = \frac{1}{2} \xi_1^2$, whose time-derivative along solutions of the first equation of (31) is given by, $\dot{V}_1 = \xi_1 (\xi_2 + v)$. Let us choose the virtual control $v = -k_1 \xi_1$, and then $\dot{V}_1 = \xi_1 \xi_2 - k_1 \xi_1^2$. Therefore, one can rewrite (31) as,

$$\begin{aligned} \dot{\xi}_1 &= \xi_2 - k_1 \xi_1 \\ \dot{\xi}_2 &= -\frac{k_p}{m_p} (\xi_1 + x_1^d) - \frac{c_p}{m_p} (\xi_2 - k_1 \xi_1 + x_2^d) \\ &\quad + \frac{d_p}{m_p} u + \Delta(x, t) - \dot{x}_2^d + k_1 \xi_2 - k_1^2 \xi_1. \end{aligned} \quad (32)$$

Let us propose $V = V_1 + \frac{1}{2} \xi_2^2$, whose time-derivative along the trajectories of (32) is given by,

$$\begin{aligned} \dot{V} &= \xi_1 \xi_2 - k_1 \xi_1^2 + \xi_2 \left(\frac{d_p}{m_p} u + \Delta(x, t) - \dot{x}_2^d + k_1 \xi_2 - k_1^2 \xi_1 \right. \\ &\quad \left. - \frac{k_p}{m_p} (\xi_1 + x_1^d) - \frac{c_p}{m_p} (\xi_2 - k_1 \xi_1 + x_2^d) \right). \end{aligned} \quad (33)$$

By substituting control (28) with coordinates (30), (33) is simplified to,

$$\dot{V} = -k_1 \xi_1^2 - k_2 \xi_2^2, \quad (34)$$

and then, $\dot{V} \leq -\sigma V$ with $\sigma = \min\{2k_1, 2k_2\}$, [18]. Therefore ξ_1, ξ_2 globally exponentially converges to zero, and then $x_1 \rightarrow x_1^d$ and $x_2 \rightarrow x_2^d$, in the same way. ■

To demonstrate that the active disturbance rejection control $u(\hat{x}_1, \hat{x}_2, \hat{\Delta})$ asymptotically stabilizes the error origin (29), we make use of Propositions 1 and 2. Notice that in Proposition 2, we assumed that all the system states (x_1, x_2) , and even disturbance $\Delta(x, t)$ are available for feedback. Accordingly, the latter is relaxed in the following active disturbance rejection control design.

Proposition 3: Let us consider: a) the conditions of Lemma 1, b) the observer of Proposition 1, and c) the

state feedback control of Proposition 2. Then, the equilibrium point (29) in closed-loop form with the feedback law $u(\hat{x}_1, \hat{x}_2, \hat{\Delta}) = u(x_1 + e_1, x_2 + e_2, x_3 + e_3)$,

$$\begin{aligned} u(\hat{x}_1, \hat{x}_2, \hat{\Delta}) &= \frac{m_p}{d_p} \left(\frac{k_p}{m_p} \hat{x}_1 + \frac{c_p}{m_p} \hat{x}_2 - \hat{\Delta} + \dot{x}_2^d \right. \\ &\quad \left. - [k_1 k_2 + 1] [\hat{x}_1 - x_1^d] - [k_1 + k_2] [\hat{x}_2 - x_2^d] \right) \end{aligned} \quad (35)$$

is globally asymptotically stable.

Proof: First, notice that the active rejection control (35) has a similar structure as (28). Thus, to simplify the notation, let us rewrite (32) and (26) as follows,

$$\begin{aligned} \dot{\xi} &= f(\xi, u(\xi + e), t) \\ \dot{e} &= F(e, u(\xi + e), t), \end{aligned} \quad (36)$$

where $\xi = [\xi_1, \xi_2]^T$, $e = [e_1, e_2, e_3]^T$, $f(\cdot)$ is the RHS of system (32), and $F(\cdot)$ is the RHS of (26). Now consider the above notation and the change of coordinates in vector form $\zeta = \xi - e$. And then, the system (36) can be rewritten as follows,

$$\begin{aligned} \dot{\xi} &= f(\xi - e, u(\xi), t) + F(e, u(\xi), t) \\ \dot{e} &= F(e, u(\xi), t). \end{aligned} \quad (37)$$

To prove that the origin of (37) converges, let us propose the candidate Lyapunov function, $\tilde{V}(\xi, e) = \kappa V(\xi) + W(e)$, where $\kappa \in \mathbb{R}_{>0}$. The derivative of $\tilde{V}(\xi, e)$ along the trajectories of (37) is given by,

$$\begin{aligned} \dot{\tilde{V}} &= \kappa \frac{\partial V(\xi)}{\partial \xi} \dot{\xi} + \dot{W}(e) \\ &= \kappa \frac{\partial V(\xi)}{\partial \xi} (f(\xi - e, u(\xi), t) + F(e, u(\xi), t)) + \dot{W}(e) \\ &= \kappa \frac{\partial V(\xi)}{\partial \xi} f(\xi - e, u(\xi), t) + \kappa \frac{\partial V(\xi)}{\partial \xi} F(e, u(\xi), t) \\ &\quad + \kappa \frac{\partial V(\xi)}{\partial \xi} f(\xi, u(\xi), t) - \kappa \frac{\partial V(\xi)}{\partial \xi} f(\xi, u(\xi), t) + \dot{W}(e) \\ &= \kappa \frac{\partial V(\xi)}{\partial \xi} f(\xi, u(\xi), t) + \dot{W}(e) \\ &\quad + \kappa \frac{\partial V(\xi)}{\partial \xi} (f(\xi - e, u(\xi), t) + F(e, u(\xi), t) - f(\xi, u(\xi), t)). \end{aligned} \quad (38)$$

According to the conditions of Lemma 1, Propositions 1 and 2, together with the change of coordinates (29) and (30), it follows that the RHS of (36) is bounded and so the RHS of (37). Therefore, $\|f(\xi - e, u(\xi), t)\|_2 \leq \varrho_1$, $\|F(e, u(\xi), t)\|_2 \leq \varrho_2$, and $\|f(\xi, u(\xi), t)\|_2 \leq \varrho_3$, with $\varrho_1, \varrho_2, \varrho_3 \in \mathbb{R}_{\geq 0}$. Furthermore, $\frac{\partial V(\xi)}{\partial \xi} f(\xi, u(\xi), t) \leq -\varrho_4 \|\xi\|_2^2$ follows from (34), with $\varrho_4 \in \mathbb{R}_{>0}$. Besides, according to [19], it follows that, $|\frac{\partial V(\xi)}{\partial \xi}| \leq \varrho_5 \|\xi\|_2$ with $\varrho_5 \in \mathbb{R}_{>0}$. Therefore, considering the above and (27), (38) can be simplified to,

$$\begin{aligned} \dot{\tilde{V}} &\leq -\kappa \varrho_4 \|\xi\|_2^2 - \varrho_6 \|e\|_1 + \kappa \varrho_5 (\varrho_1 + \varrho_2 + \varrho_3) \|\xi\|_2 \\ &\leq -(\kappa \varrho_4 \|\xi\|_2 - \kappa \varrho_5 (\varrho_1 + \varrho_2 + \varrho_3)) \|\xi\|_2 - \varrho_6 \|e\|_1. \end{aligned} \quad (39)$$

where $\varrho_6 \leq a$. Thus, following the procedure similar to [20] and [21], it follows that the equilibrium point (ξ, e) globally

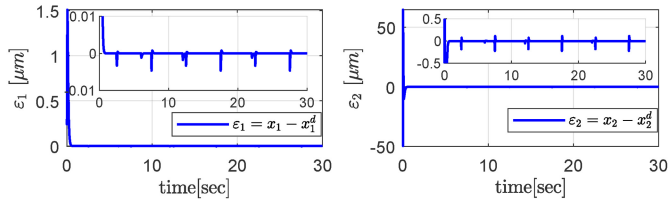


Fig. 2. The tracking errors (29) under the proposed control and a zoom near zero. $y = x_1$ is the only available output.

asymptotically converges to zero, and thus, the Σ_1 trajectories in closed-loop form with $u(\hat{x}_1, \hat{x}_2, \hat{\Delta})$ converge to the desired trajectories (x_1^d, x_2^d) in the same way. ■

IV. SIMULATION RESULTS

The system parameters used for simulation correspond to the actuator in [14] with hysteresis model of [16]. The desired trajectory is $x_1^d = 80 \sin \frac{2\pi}{10} t$ with first-time and second derivatives, $\dot{x}_1^d = x_2^d$ and $\ddot{x}_1^d = \dot{x}_2^d$, respectively.

The closed-loop system response under the effect of the proposed control (35) is depicted in Fig. 2. There are slight differences near zero in the non-differentiable points of Δ due to the minor differences in its estimate $\hat{\Delta}$ on those points.

The simulation details are in our supplementary material and include the following:

- System and control parameters.
- Several graphs of all the system states and their estimates.
- Comparison with state-of-the-art controllers.
- Simulation under parameter variations.
- The control input-output hysteresis loop.

V. CONCLUSION

In this letter, we proposed to design a feedback controller by using the hysteresis model of a piezoelectric actuator used as a digital manipulator. Since the hysteresis was assumed to be non-symmetric, the Dahl model was proposed. We first analyzed the complete system behavior given by system Σ with bounded inputs to solve the control problem. It was demonstrated that all the system trajectories under the above conditions are bounded. This result permits us to design an observer for part of the entire system given by Σ_1 . Furthermore, this observer throws estimates of the position and velocity terms together with the exogenous disturbances and non-linearities depending on the unobservable subsystem Σ_2 . Once the observer is designed, a controller is synthesized using the estimated states for feedback. Finally, we proved the global asymptotic stability of the error equilibrium point.

On the one hand, future works include the experimental test of the proposed control law on a benchmark based on a piezoelectric actuator. On the other hand, the control law needs a sensor that measures the output displacement of the actuator. In practice, it is challenging to implement a sensor to measure this displacement due to the limited space within the robotic hand. Therefore, another perspective is implementing

piezoelectric self-sensing in the actuator, allowing it also to be a sensor of its displacement [22].

REFERENCES

- [1] L. S. Mattos et al., “ μ RALP and beyond: Micro-technologies and systems for robot-assisted endoscopic laser microsurgery,” *Front. Robot. AI Sect. Biomed. Robot.*, vol. 8, Sep. 2021, Art. no. 664655.
- [2] F. J. Salvador, A. H. Plazas, J. Gimeno, and M. Carreres, “Complete modelling of a piezo actuator last-generation injector for diesel injection systems,” *Int. J. Engine Res.*, vol. 15, pp. 3–19, Sep. 2012.
- [3] C. Y. Kiyono, P. H. Nakasone, J. Yoo, L. A. M. Mello, and E. C. N. Silva, “On the optimization of HDD arms with piezoelectric actuation,” *Finite Elements Anal. Des.*, vol. 88, pp. 118–127, Oct. 2014.
- [4] G. Binnig, C. F. Quate, and C. Gerber, “Atomic force microscope,” *Phys. Rev. Lett.*, vol. 56, pp. 930–933, Mar. 1986.
- [5] D. Habineza, M. Rakotondrabe, and Y. L. Gorrec, “Multivariable generalized Bouc-Wen modeling, identification and feedforward control and its application to multi-DoF piezoelectric actuators,” in *Proc. IFAC World Congr.*, 2014, pp. 10952–10958.
- [6] M. Rakotondrabe, “Multivariable classical Prandtl-Ishlinskii hysteresis modeling and compensation and sensorless control of a nonlinear 2-DoF piezoactuator,” *Nonlinear Dyn.*, vol. 89, pp. 481–489, Mar. 2017.
- [7] R. Oubellil, Ł. Ryba, A. Voda, and M. Rakotondrabe, “Experimental model inverse-based hysteresis compensation on a piezoelectric actuator,” in *Proc. Int. Conf. Syst. Theory Control Comput.*, 2015, pp. 186–191.
- [8] Y. Cao and X. B. Chen, “A survey of modeling and control issues for piezoelectric actuators,” *J. Dyn. Syst. Meas. Control*, vol. 137, no. 1, 2015, Art. no. 14001.
- [9] D. Devasia, E. Eleftheriou, and S. O. R. Moheimani, “A survey of control issues in nanopositioning,” *IEEE Trans Control Syst. Technol.*, vol. 15, no. 5, pp. 802–823, Sep. 2007.
- [10] G.-Y. Gu, L.-M. Zhu, C.-Y. Su, H. Ding, and S. Fatikow, “Modeling and control of piezo-actuated nanopositioning stages: A survey,” *IEEE Trans Autom. Sci. Eng.*, vol. 13, no. 1, pp. 313–332, Jan. 2016.
- [11] G. Flores and M. Rakotondrabe, “Robust nonlinear control for a piezoelectric actuator in a robotic hand using only position measurements,” *IEEE Contr. Syst. Lett.*, vol. 6, pp. 872–877, 2022.
- [12] G. Flores, N. Aldana, and M. Rakotondrabe, “Model predictive control based on the generalized Bouc-Wen model for piezoelectric actuators in robotic hand with only position measurements,” *IEEE Contr. Syst. Lett.*, vol. 6, pp. 2186–2191, 2022.
- [13] G. Flores and M. Rakotondrabe, “Finite-time stabilization of the generalized Bouc-Wen model for piezoelectric systems,” *IEEE Contr. Syst. Lett.*, vol. 7, pp. 97–102, 2022.
- [14] Q. Xu and Y. Li, “Dahl model-based hysteresis compensation and precise positioning control of an XY parallel micromanipulator with piezoelectric actuation,” *J. Dyn. Syst. Meas. Control*, vol. 132, no. 4, pp. 1–12, 2010.
- [15] S. K. Shome, M. Prakash, S. Pradhan, and A. Mukherjee, “Robust dahl model based sliding mode control for micro/nano positioning applications,” in *Proc. Annu. IEEE India Conf. (INDICON)*, 2014, pp. 1–6.
- [16] S. Khadraoui and M. Rakotondrabe, “Characterization and RST control of a nonlinear piezoelectric actuator for a robotic hand,” in *Proc. Joint Symp. Mechatronic Syst. IFAC Conf. Motion Vib. Control*, 2022, pp. 428–433.
- [17] D. Helmick and W. Messner, “Higher order modeling of hysteresis in disk drive actuators,” in *Proc. 42nd IEEE Int. Conf. Decis. Control*, vol. 4, 2003, pp. 3712–3716.
- [18] G. Flores, “Longitudinal modeling and control for the convertible unmanned aerial vehicle: Theory and experiments,” *ISA Trans.*, vol. 122, pp. 312–335, Mar. 2022.
- [19] N. Krasovskiy, *Some Problems of Stability of Motion Theory*, 1st ed. Moscow, Russia: Fizmatgiz, 1959.
- [20] G. Flores and M. Rakotondrabe, “Output feedback control for a nonlinear optical interferometry system,” *IEEE Contr. Syst. Lett.*, vol. 5, pp. 1880–1885, 2021.
- [21] A. E. Golubev, A. P. Krishchenko, and S. B. Tkachev, “Separation principle for a class of nonlinear systems,” in *Proc. IFAC World Congr.*, vol. 35, 2002, pp. 447–452.
- [22] M. Rakotondrabe, “Combining self-sensing with an unknown-input-observer to estimate the displacement, the force and the state in piezoelectric cantilevered actuator,” in *Proc. Amer. Control Conf.*, 2013, pp. 4523–4530.